Missouri University of Science and Technology

Scholars' Mine

Electrical and Computer Engineering Faculty Research & Creative Works

Electrical and Computer Engineering

01 Jan 2005

A New Test Setup and Method for the Calibration of Current Clamps

David Pommerenke
Missouri University of Science and Technology, davidjp@mst.edu

Ramachandran Chundru

Sunitha Chandra

Follow this and additional works at: https://scholarsmine.mst.edu/ele_comeng_facwork

Part of the Electrical and Computer Engineering Commons

Recommended Citation

A New Test Setup and Method for the Calibration of Current Clamps

David Pommerenke, *Senior Member, IEEE*, Ramachandran Chundru, *Member, IEEE*, and
Sunitha Chandra, *Member, IEEE*

Abstract—Current probes are widely used to measure the common mode currents in electromagnetic compatibility (EMC) applications. Often, it is necessary to characterize the ratio of measured voltage to the common mode currents up to gigahertz (GHz) frequencies. Existing calibration methods for current probes suffer from the problem of not directly measuring the current within the current clamp. Instead they either reconstruct the current from measurements at other locations or they use assumptions regarding the geometry which allows them to use a current that is measured at a different location without applying a mathematical correction. For example, by maintaining a 50-Ω transmission-line impedance the current can be determined with low uncertainty. The proposed method overcomes these disadvantages by directly measuring the current at the center of the current clamp. This way the mechanical dimensions of the test setup are not critical anymore, i.e., one setup can be easily used to measure a large variety of clamps. The method is primarily applicable for current monitoring probes in the frequency domain.

Index Terms—Calibration, current clamp, current probe, transfer function, transfer impedance.

I. INTRODUCTION

CURRENT probes are used in many electromagnetic compatibility (EMC) applications, for example, to identify the sources of radiation [1] or as injection probes to emulate the coupling of fields to wires [2]. Limiting the analysis to the application as current monitoring probes, the transfer impedance Z_{trans} is the most important parameter

$$Z_{\text{trans}} = \frac{V_{\text{clamp}}}{I_{\text{wire}}^*}. \tag{1}$$

where V_{clamp} is the output voltage of the clamp loaded with 50 Ω in most cases and I_{wire}^* is the current that is flowing in the wire at the center of the clamp.

As attaching the current clamp will influence the measured currents through mechanisms discussed later in more detail, a second definition is possible, while not often used

$$Z_{\text{trans}} = \frac{V_{\text{clamp}}}{I_{\text{wire}}} \tag{2}$$

where I_{wire} is the current that is flowing in the wire before the current clamp was mounted.

The difference between both definitions diminishes if the effect of the current clamp on the current is negligible and it mirrors discussions around the optimization of oscilloscope probing in > 3-GHz bandwidth for signal integrity applications.

In a first approximation, the loading of the probe can be understood using a transformer model [3]. Here the loading effect is modeled as series impedance within the wire the probe is attached to. The transformer model is only valid at low frequencies for two reasons: the parasitics internal to the probe require the use of a complex equivalent circuit [4]–[7] and the probe body scatters the field that is propagating along the wire [3], thus, it influences the current on the wire beyond the influence of the transformed impedance. The situation is further complicated by currents on the cable that connects to the probe. Exact analytical derivation for the transfer impedance based on details of the construction is not obtainable for any but the simplest cases. Consequently, there is need for the characterization of the probes up to gigahertz (GHz) frequencies via experimental methods.

Different methods are in use or have been proposed for the characterization.

- **CISPR**: Probably the most widely used method is described by CISPR [8] that is similar to [2]. A coaxial line is built, such that the current clamp forms part of the return current path. If careful impedance matching is used, the current can be either obtained from the source voltage and the characteristic impedance, or as a first step in improvements, from the output voltage of the transmission line.

- **Ruddle et al.**: The CISPR method requires a special test fixture for each current clamp for achieving the 50-Ω match. Improving beyond this, Ruddle *et al.* [9] proposed a method that allows for the mismatches between the 50-Ω transmission lines and the transmission line that is formed by the current clamp but takes them mathematically into account.

- **Cerri et al.**: A further, very interesting improvement of the method is provided by Cerri *et al.* [3]. On the one side, they realized that the test setup used by Ruddle *et al.* could be modified for allowing a simpler characterization, on the other, they wanted to measure the current clamp in a geometry that is closer to the geometry of its real application. As such the complete setup, current clamp around a cable above ground, is taken as one unit to incorporate the field scattering effects of the current clamp
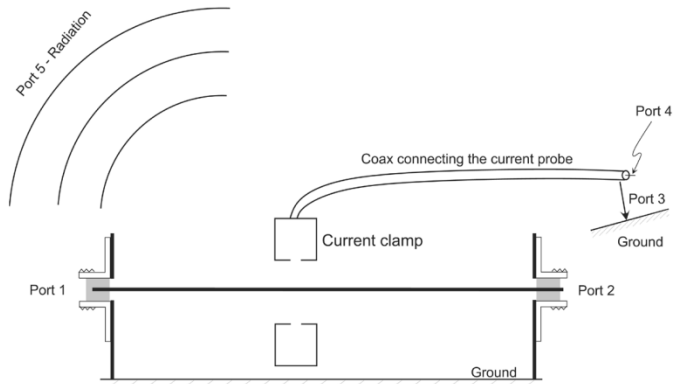
Fig. 1. Five ports that describe a calibration setup for current clamps.

Fig. 2. Calibration setup for current clamps using a series resistor to measure the current.

Fig. 3. Detail of the current sensing resistor and the gap. The inner conductor of the transmission line B is soldered to the solid rod.

and other second-order effects. Input and output S-parameters and time-domain data are recorded. The setup is analyzed as a chain connection of transmission lines and, after data correction, the transfer impedance is obtained in a wide frequency range. The data correction includes unifying low-frequency data obtained from S-parameters with time-domain data that provides better accuracy at high frequencies. The method provides a set of S-parameters that also characterizes the effect of the probe on the wire to which it is attached.

All of the methods mentioned above follow the concept of taking an imperfect measurement setup and improving the data by mathematical correction with increasing complexity. In an expansion of the 3-port equivalent circuit chosen in [3] a 5-port equivalent circuit may be chosen purely for the purpose of illustrating the complexity faced by a mathematical correction (Fig. 1). The 5-ports are given as follows:

- port 1, port 2, and port 4 provide the coaxial connection to the NWA;
- port 3 expresses the waves that flow on the outside of the coax cable that connects the probe to the NWA;
- port 5 expresses the radiation from different parts of the structure and waves that pass by the side of the plates that usually hold the port 1 and port 2 connectors.

The basic drawback of these methods comes from the way the current within the clamp is obtained. Instead of a direct measurement, it needs to be reconstructed using data measured somewhere else. In case the method described by CISPR is used, the geometry must be adapted to each clamp by maintaining a 50-Ω transmission-line impedance as best as possible, in order to determine the current with low uncertainty. The proposed method overcomes these disadvantages by directly measuring the current at the center of the current clamp. This way the mechanical dimensions of the test setup are not critical anymore, i.e., one setup can be easily used to measure a large variety of clamps.

In contrast, our approach optimizes the test setup to a point at which no data correction is needed anymore but still allows taking a setup that is close to the real application.

After the introduction, the mechanical arrangement of the calibration method is explained in Section II. The measurement procedure is explained in Section III. The performance of the calibration method analyzed in Sections IV and V presents a more general discussion on secondary parameters that influence the accuracy of current clamp measurements.
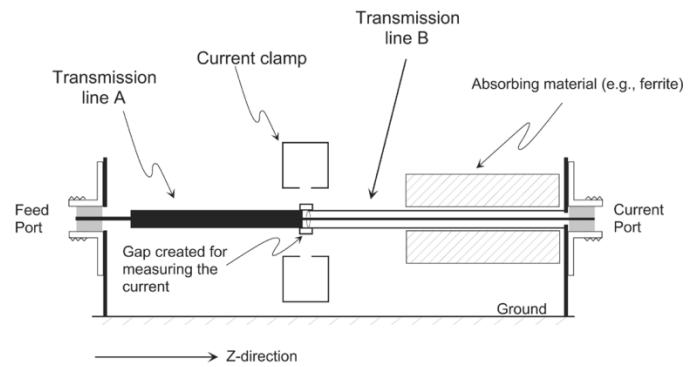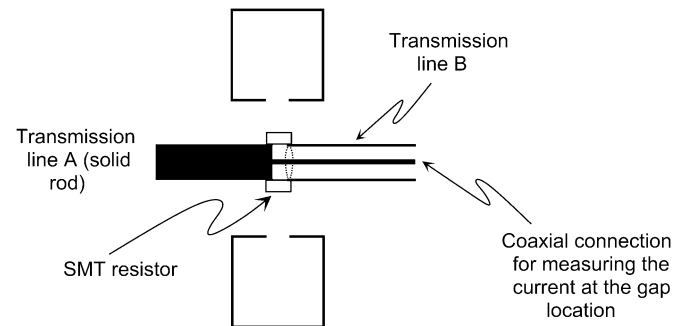
II. MECHANICAL ARRANGEMENT

The current clamp is placed around a wire that carries a current. The current in the wire and the output voltage of the clamp are measured. The setup is shown in Fig. 2 and the details at the current clamp position in Fig. 3

As shown in Figs. 2–4 only the inner conductor of the semirigid coax cable (transmission line B) is connected to the rod of the transmission line system A. Disregarding the displacement current, we see that the current which flows on the "center" conductor of transmission line system A must flow via the low impedance sensing resistor to reach transmission line B. The current is obtained from the voltage drop across the sensing resistor taking into account that from a current's perspective the sensing resistor is in parallel with the terminated 50–Ω impedance of the current port.

This setup comprises the following elements shown in Figs. 2, 3, and 5.

- A feed port for creating the current for injecting a signal.
- A transmission line A from the feed port to the gap. The transmission line is formed by a solid rod above a ground plane. Here, the shield of a semirigid cable is used. If one desires, the geometry of the wire-above-ground structure can be chosen to be similar to the real application of the current probe.
- A gap between two transmission lines (Gap). The gap allows measuring the current using a sensing resistor. The
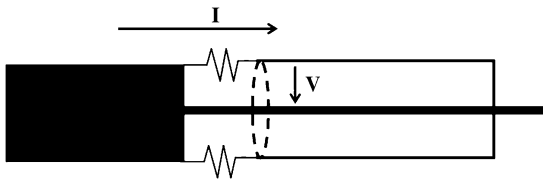
Fig. 4.   Detail of the current sensing resistor, the current and the detected voltage. The inner conductor of the left coax is soldered to the center of the rod that is shown on the right side.

Fig. 5.   Photo of the large test setup. The ferrites form an absorbing structure. Having a few clamp-on ferrites provides sufficient absorption.

Fig. 6.   Detail of the current sensing resistor made from a circular arrangement of SMT resistors.

sensing resistor is composed of 30 surface mounted resistors of size 0805 (80 × 50 mil) placed around the circumference of the gap to form a low inductance resistor (Figs. 4 and 6). The resistance values are in the range of 1–10 Ω. Assuming a frequency independent real resistance, the current is given directly by the voltage measured at the "current port." The value of the shunt resistance should not be too low (e.g., 1 Ω may be too low) due to the difficulties in constructing a frequency independent current sensing resistor. If its value is too low, then the mutual inductance caused by magnetic flux leaking from the outside of the resistor ring into the inside would lead to a frequency dependence. The current sensing resistor would have a significant series inductive component. Its value should also not be too large either, as the longitudinal E-field will cause a displacement current. The magnetic field of the displacement current is also measured by the current clamp, but the displacement current would not be measured by the current sensing resistors, leading to a systematic error. The ratio of displacement to conduction current will depend in first order on the ratio of the current sensing resistance to the impedance of the transmission lines A and B.

Part of the forward traveling wave will be reflected as it encounters the current shunt resistor. The reflection is quite small. For the large setup the sensing resistor value is 4.82 Ω, placed in series with a 185-Ω transmission line. The reflection coefficient is just above 1%. Only a small systematic error will be introduced.

- A second transmission line (transmission line B) forms two transmission line systems: An inner one (made from a semirigid cable) that is used to connect the gap to the current port and an outer transmission line between the shield and the ground plane. Although not necessary for the function of the test method, the outer transmission line has the same cross section as the transmission line from the feed port to the gap.
- A current clamp positioned above the gap.
- An absorbing structure placed on transmission line B. The purpose of the absorbing structure is to reduce the current standing wave ratio (CSWR) on the transmission lines A, B and in the gap region. As the current is measured via the current port, the absorbing elements do not have to be providing a good match. They are mainly there to avoid current-nulls or large current gradients (dI/dz) that might occur at the position of the current clamp if the CSWR were to be large. Further details are analyzed in the discussion section.
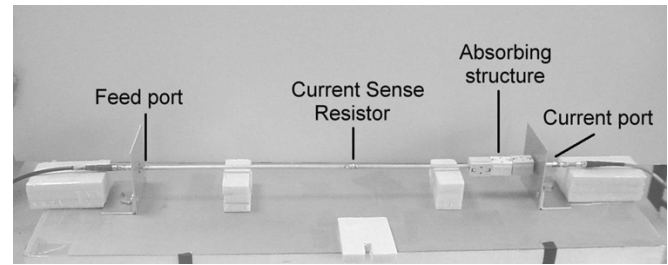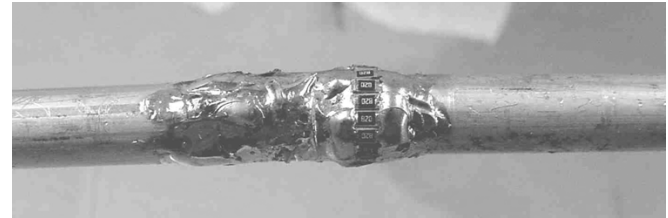
- A port to measure the current (current port).

Fig. 5 shows a photo of one of the two setups constructed ("large" setup). It has been constructed from a low loss 1/4-in semirigid coax cable. The characteristic impedance of the transmission line A and the outer transmission line system of transmission line B was determined to be 185 Ω from the dimensions of the structure.

A detailed photo of the current sensing surface mounted resistors is shown in Fig. 6. The resistors are arranged in a circular fashion to minimize the inductive coupling between the current flowing on the outside and current sensing voltage loop on the inside. It has been shown in [10], [11] that a broad-band current sensing resistor can be formed using similar arrangements. For example, using a radial arrangement a transfer impedance variation of the ESD current target of less then ±0.8 dB up to 4 GHz was created at only 2-Ω resistance value for the purpose of measuring ESD currents [10], [11]. The radial arrangement minimizes the mutual inductance between the current driving and the current sensing sides of the current shunt [12].

It is worth noting the following:

- the feed does not have to be very precise, neither the transition from the coax to transmission line A nor do both transmission lines have to have the same cross section;
- the requirement for absorption by the ferrites is not a strong requirement;
- the geometry of the cross sections (i.e., the impedances of the transmission lines) is not critical.

For showing the generality of the design, two test setups have been built that differ significantly in their geometry, their sensing resistor values and their characteristic impedances. A summary of the main parameters of both test setups is given in Table I. Besides the differences in impedances, variations of the absorption schemes have been performed. The resistances have been determined using 4-wire-4-contact point measurements (HP4263B) [13].

TABLE I
MAIN PARAMETERS OF THE TWO SETUPS AND THEIR TRANSMISSION
LINES (TL)

	"large" setup	"small" setup
TL height / diameter	51 mm	51 mm
	6.35 mm	2.2 mm
TL impedance	185 Ω	240 Ω
Sensing resistor	4.8 Ω	9.3 Ω
Setup length	610 mm	410 mm
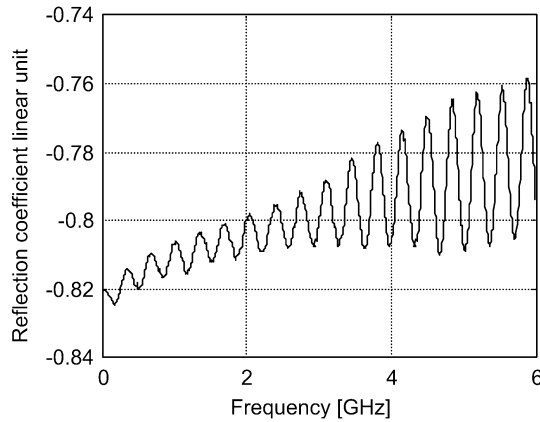
Fig. 7.   Reflection coefficient as seen from the current port side (feed port is open circuited).

Fig. 8.   Transmission line equivalent circuit for the setup shown in Figs. 2 and 5.

To verify the quality of the sensing resistor and its connections the reflection coefficient, as seen from the current port, has been measured. It is shown in Fig. 7.

The data shown in Fig. 7 indicates a good mechanical design:

*   at low frequencies the reflection coefficient is determined by the dc resistance of 4.8 Ω;
*   with increasing frequency, the reflection coefficient increases in average.
*   an undulation of the reflection coefficient is visible.

The undulation of the reflection coefficient is caused by multiple reflections between the SMA connector and the current sense resistor. The semirigid coax cable has an impedance of 50.8 Ω; its connection to the SMA shows an extra series inductance of about 40 pH. The increase of the reflection coefficient is caused by the loss of the connecting coax cable, as the loss leads to an improved match.

III. MEASUREMENT PROCEDURE

The probes are typically characterized in a two step process, although a single step process is possible, if the Reference, Channel A and Channel B ports of the network analyzer are accessible. Here, only the two step method is described. Briefly, the first step (measurement #1) will determine the current within the clamp and the second step (measurement #2) determines the output voltage of the clamp. In the data analysis, the ratio of the measurements is taken to determine the transfer impedance. The analysis of the "large" setup leads to an equivalent circuit as shown in Fig. 8.

A. Measurement # 1: Characterization of the Current

A network analyzer is connected to the "feed port" and the "current port." The current clamp is positioned above the gap and terminated with 50 Ω. The cabling to the current clamp is in its final position. The S_{21} measurement "S_C" will determine the current in the gap, i.e., the current at the center of the current clamp. As seen from Fig. 8, the current needs to be determined as the voltage drop across the parallel connection of the current sensing resistor and the 50-Ω load at the "current port."

As this is an open setup, it is easy to perform additional manipulations to obtain an insight into the effect of secondary parameters. Possible examples are the following:

*   the effect of the current clamp on the current can be seen by removing the current clamp and observing the changes at the "current port;"
*   the effect of the current clamp cable routing, grounding or ferrite loading can also be seen by observing the changes at the "current port."

B. Measurement # 2: Characterization of the Current Clamp Output Voltage

In the second step, the termination is moved to the "current port" and port 2 of the network analyzer is connected to the current clamp. This S_{21} measurement (S_V) will determine the output voltage of the current clamp. A complex transfer impedance can be determined from the complex S_{21} data by shifting the phase reference plane from the calibration plane (at the "current port") along the semirigid cable to the position of the current sensing resistor. As a short low-loss cable had been selected, we can reasonably assume a loss-less transmission line, thus, only a correction of the phase is needed.

Again, the open nature of the structure allows additional experiments that might be of interest:

*   effect of the current clamp position (in Z-direction) on the output voltage;
*   effect of placing the current sensing resistor offcenter of the current clamp;
*   effect of tilting the current clamp;
*   effect of inverting the direction of the current clamp (every difference between the directions of the current clamp,
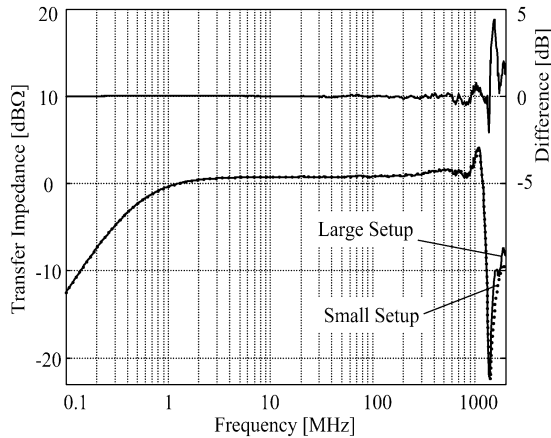
Fig. 9. Comparison of the transfer function obtained in the "large" and the "small" calibration setups. The top trace indicates the difference and is referenced to the Y axis on the right side.

Fig. 10. Current passing through the current sensing resistors relative to 1-V source voltage of the network analyzer.

other than a phase change, indicate capacitive coupling to the inside of the current clamp).

C. Data Processing

The magnitude transfer impedance Z_{trans} expressed in dBΩ is obtained from the data sets S_C and S_V and the resistance of the sensing resistor R_{sense} using

$$Z_{\text{trans}} = S_V - S_C + 20 \cdot \log_{10}\left(\frac{R_{\text{sense}} \cdot 50}{R_{\text{sense}} + 50}\right). \quad (3)$$

IV. PERFORMANCE

The performance of the method is shown in three steps. The first two steps show the self consistency of the method. That is, the independence of the transfer impedances obtained from the characteristic impedance of the setup (Section IV-A.1) and an negligible influence of the termination method (Section IV-A.2).

Finally, the transfer impedances obtained by this method are compared to another method that uses a highly controlled geometry.

1) Independence of the Transfer Impedance From the Impedance of the Test Setup: We start by contrasting this approach to the CISPR [8] approach. The widely used CISPR method requires maintaining a 50-Ω transmission-line impedance, forcing the user to design different test setups for different current clamps. This setup overcomes this limitation, as do the methods proposed in [3], [9], although not explicitly shown.

To verify this claim, the same F-65 current clamp was measured in the "large" and the "small" test setups. The results shown in Fig. 9 indicate that the differences are less then ± 0.3 dB for frequencies within the manufacturer specified operating range of 100 kHz–1 GHz. This experimental data supports the claim of being able to characterize the transfer impedance of the probe independent of the geometry of the test setup.

2) Independence of the Transfer Impedance From the Termination Method: Another important property of this test setup is
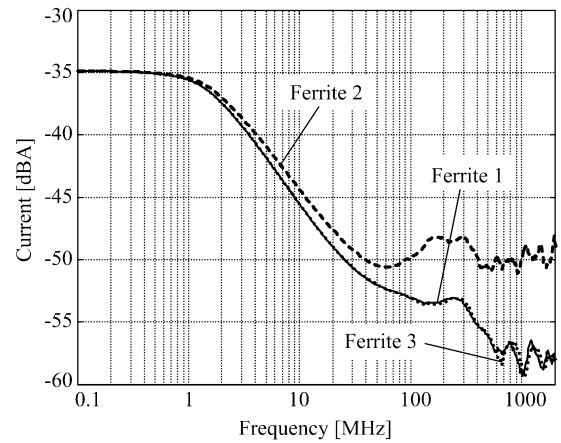
that no good match needs to be obtained for the wave on the outside of the transmission lines B as it encounters the metal plane at the "current port." Of course, the termination will affect the current passing through the clamp, but as this is exactly measured at the probe location, the variation of the current will be removed by taking the ratio to the voltage at the current clamp.

However there are limits to this approach; a termination cannot be totally avoided for the following two reasons.

1) If the CSWR would reach infinity, then there could be a current null at the position of the current clamp. This needs to be avoided as very low current values would increase the sensitivity to noise and small geometry variations that would move the position of the current null.

2) If the gradient of the current (dI/dz) is too strong the exact position of the current clamp starts to influence the measured current and the definition of the current clamp transfer impedance weakens. The discussion section analyzes this further.

Still, the resulting requirement for termination is not strong. In practice, a few ferrites will be sufficient. They do not have to be effective absorbers at lower frequencies, as long as the distance between the current port and the sensing resistance is less than $\lambda/4$. Below this frequency, the short of the transmission line B cannot be transformed into an open. If this could happen, then too small a current would be flowing through the sensing resistor. Using typical dimensions of 30 cm shows that the termination does not have to be effective below 150 MHz. A further enhancement is possible by placing ferrites onto transmission line A, close to the feed port. These ferrites will partially absorb energy that is reflected by the current probe's body, thus, reducing the current gradient. The resulting reduction of the available power by a few decibels (Fig. 10) in the measurement system will not affect the uncertainty of the measurement as the difference between two measurements is taken.

Three different ferrite arrangements have been used on the "large" setup. The effect of the ferrites on the measured current is shown in Fig. 10.

An F-65 (Fischer Custom Communications) current clamp was used while the absorbing structure was varied. Setups "ferrite 1" and "ferrite 3" have a different number of ferrites at the
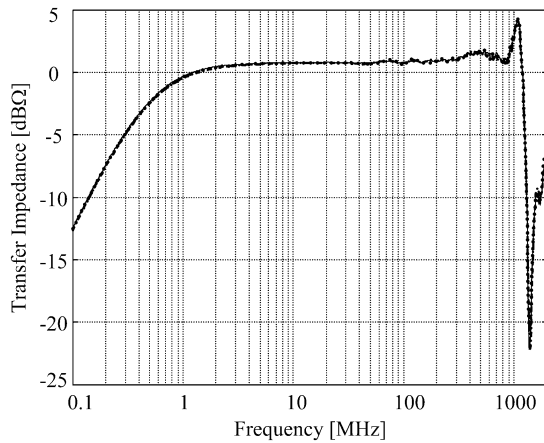
Fig. 11. Comparison of the transfer function using different absorbing structures at the current port and the feed port.
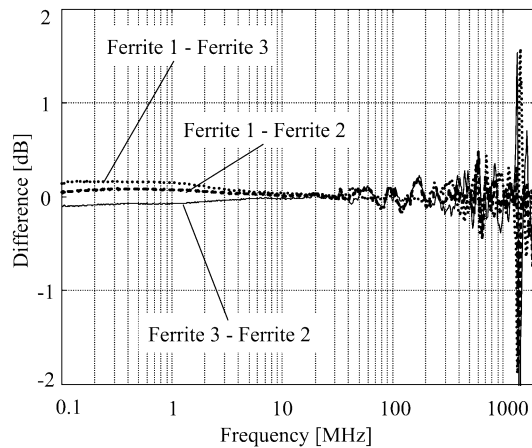
Fig. 12. Differences in the transfer function obtained by varying the absorbing structures.

current port and the same number of ferrites at the feed port. Setup "ferrite 2" is similar to "ferrite 1" except that it has no ferrites at the feed port. As one would expect, the largest difference is seen if a ferrite is placed at the feed port (Fig. 10). Setup "ferrite 2" has the worst standing wave ratio, as reflections between 100–1000 MHz become visible as undulations of the current magnitude.

The voltage output of the current clamp was measured for these ferrite arrangements and the transfer impedance calculated. The results shown in Figs. 11 and 12 support the claim of independence from the absorbing structure. The differences between the transfer impedances are minimal, less than ± 0.4 dB within the design range of the current clamp (100 kHz–1 GHz).

For improved visualization, the differences are plotted in Fig. 12. As can be seen, the difference in the transfer functions is very small up to 1 GHz, which is at the higher end of the F-65 current probe's usable frequency range. Larger deviations occur at resonance frequencies of the clamp, most likely due to small shifts in the resonance behavior that are enhanced by taking the difference.

3) Comparison With Other Methods: A method that uses a highly controlled geometry was chosen as a reference method (Fig. 13). Here a current clamp can be calibrated by placing it
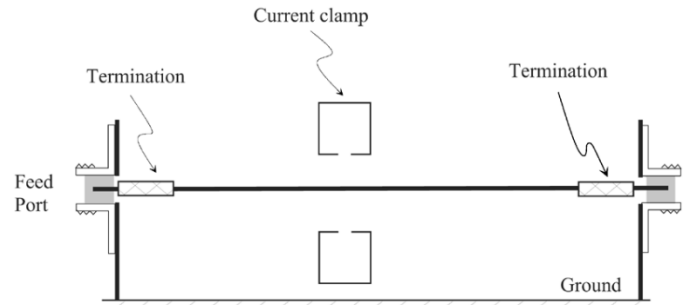
Fig. 13. Calibration of a current clamp in a well-matched transmission line system.
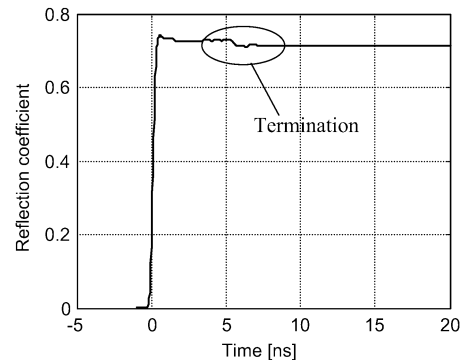
Fig. 14. Input reflection coefficient of the termination. Measured by removing the termination at the feed port using 3-GHz bandwidth (Hp 8753D network analyzer).

around a transmission line that is well terminated at both ends (Fig. 14). The method was selected since it can be at least partially analyzed analytically and as the absence of multiple reflections can be verified by moving the current clamp along the wire.

Using an S11 measurement the system was matched as good as possible (Fig. 14). The symmetric system had a 290-Ω characteristic impedance, the matching structures consisted of resistors having a total of 240 Ω distributed over a length of about 1/2 the height and a 50-Ω coaxial transition. Using terminations on both sides reduces standing waves that might be caused by reflections on the body of the current clamp.

The current, that is needed to reference to the clamp output voltage is obtained as the average of three data sets: 1) the current calculated from the source voltage and the input reflection; 2) from the current that would flow at low frequencies if a 50-Ω system feeds into a 580-Ω termination; and 3) from the current that was measured at the far-end termination. The differences of the currents indicate an uncertainty of 3 dB at 1 GHz and less below.

Results for both methods (Fig. 15) indicate the difference is less than 2 dB for the operational range of the current clamp. The remaining differences are possibly caused by the lack of exact current information in the matched wire method.

4) Application to Higher Frequencies: As another example, going up to higher frequencies the F-2000 current clamp was measured in both test setups. The transfer impedance is shown in Fig. 16.

Both setups yield similar results, i.e., the differences are less than ± 0.5 dB up to 1 GHz and less than ± 2 dB up to 3 GHz.
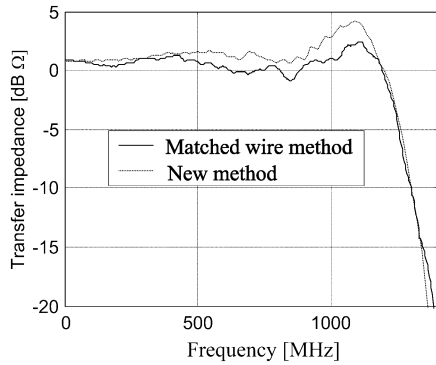
Fig. 15. Comparison of the transfer impedances measured using the proposed method (large setup) and the matched wire setup.
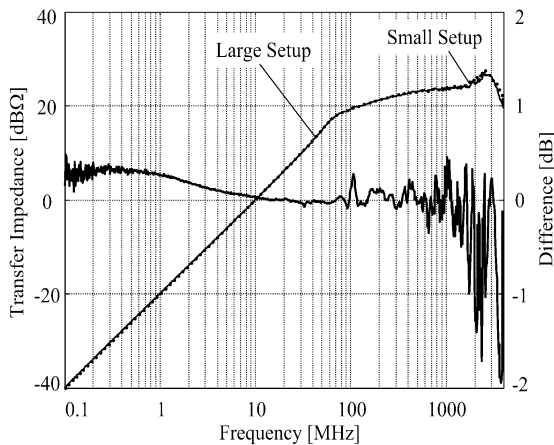
Fig. 16. Comparison of transfer impedances obtained on the "large" and the "small" setup for the F-2000 (Fischer Custom Communication) current clamp. The difference is referenced to the Y axis on the right side.

Multiple factors may contribute to these differences. The inner diameter of the F-2000 current probe is only 13 mm while the outer diameter of the sensing resistors is 8.5 mm for the large and 4 mm for the small setup. This leaves only a small gap, increasing the difficulty of centric placement. Further, the CSWR may cause sensitivity with respect to the longitudinal placement, as detailed in the discussion section. Overall, the data shown in Fig. 16 indicate the usefulness of the proposed method at frequencies beyond 1 GHz.

V. DISCUSSION

Current clamp measurements are affected by a multitude of secondary parameters. In practice, it is important to consider them if the uncertainty of the measurement is estimated or formally calculated. Significant ones are related to currents flowing on the cable that is attached to the clamp, the exact positioning of the wire through the clamp and the effect of the CSWR. Most these influences are caused by the coupling between the wire and the current clamp's enclosure, remaining capacitive coupling to the internal wiring and an internal construction that does not provide symmetry of revolution.

Offcenter and Tilting

Throughout the previous sections we assumed that that the wire passes through the center of the current clamp and that
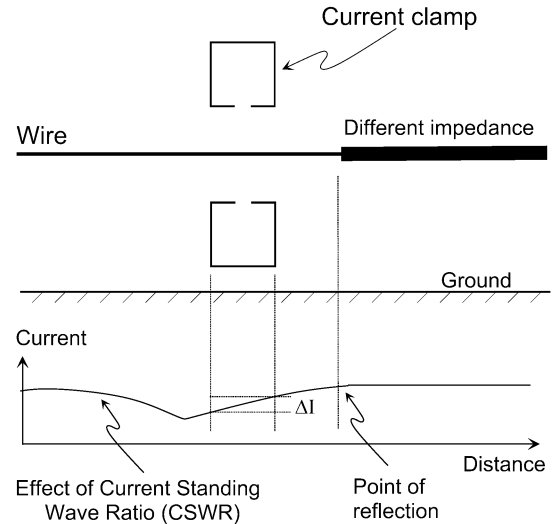
Fig. 17. Effect of CSWR on the current through a current clamp. The CSWR will cause a current difference ΔI between the left and the right side of the current clamp.

the current clamp is not tilted. While this is generally achieved during calibration it is not the case in most measurements. The open nature of the setup allows obtaining an insight into these effects, such that the user could take them into an uncertainty calculation. Offcentered wire placement or tilting of the probes varied the transfer impedance in the range of ± 0.6 dB up to 1 GHz and larger values above for the F-65 current clamp.

In theory, the current clamp should not influence the fields and from Ampere's law, it should not matter where the current passes through the current clamp. But as additional currents are introduced on the clamps body their magnetic fields will couple to the internal structure of the clamp influencing the reading. Further analysis of this coupling is beyond the scope of the article, however, it can be summarized that the transfer impedance can be determined within ± 1 dB up to 1 GHz and with larger uncertainty up to a few gigahertz.

CSWR

At first it will be shown that the CSWR limits the ability to define a unique Z_{trans}. Let us imagine the case of two transmission lines having distinct characteristic impedances joined shortly after the current clamp (Fig. 17).

For the following assumptions:

- 3-GHz frequency;
- the current clamp acts as ideal current observer, i.e., we ignore the additional effects of scattering at the body of the current clamp;
- CSWR $= 1 : 3$.

A distribution of the current along the line will be obtained as shown in Fig. 18.

To our surprise the current varies by more than 1:2 throughout the 20-mm width of the current clamp. Typically, when using the transfer impedance one does not specify in detail at which spot of the wire the current is measured. But as shown in Fig. 18, this question is of relevance. One could define it as average between the current to the left and to the right, or as the current exactly underneath the current sensing slot. As further factors contribute to the reading, such as none perfect TEM structure of the fields,
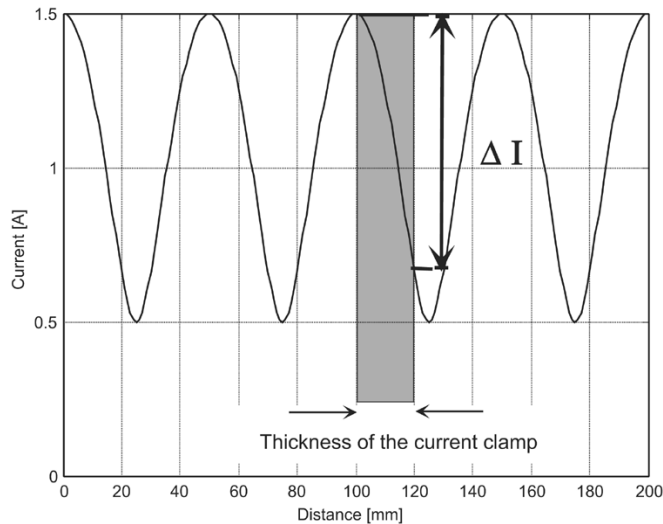
Fig. 18.   Effect of CSWR on the current along the thickness of a current clamp for the parameters shown above.

possible higher order modes on the current clamp body, tilting of the current clamp etc. it is arguable that no further detailing of the analysis will provide an improved Z_{trans} as long as the dimensions of the current clamp are not significantly reduced.

In this case the clamp had a width of 0.2 λ which led to an additional uncertainty of ± 3 dB. For practical applications we need to accept that if the current clamp width is not narrow relative to the wavelength the CSWR it will introduce an additional uncertainty that may reach many decibels.

VI. CONCLUSION

A new method for the calibration of current clamps has been developed that allows determining the transfer impedance independent of the geometry of the calibration setup. Its fundamental advantage over previous methods is that it measures the current directly at the position of the current clamp. This greatly reduces the need for data correction and provides a simple test setup that can be used for a variety of current probes.

Its main characteristics are the following:

- the method is primarily applicable for current monitoring probes in the frequency domain;
- the geometry of the setup is not a critical design parameter;
- the requirement for wave termination is not a strong;
- the setup is suitable for calibrating a multitude of current clamps, as the dimensions of the current clamp (outer diameter, inner diameter, and thickness) are not used to establish a specific impedance of a transmission line;
- the method is able to determine the complex transfer function;
- the setup is an open setup, i.e., this allows varying many secondary parameters for observing their influence. Examples are offcentered current clamps, tilting of the current clamp, ferrite loading of the current clamp coax cable etc.

REFERENCES

[1] D. C. Smith, "Current probes, more useful than you think," in *Proc. IEEE Int. Symp. Electromagnetic Compatibility*, 1998, pp. 284–289.
[2] *Road Vehicles-Electrical Disturbance by Narrow-Band Radiated Electromagnetic Energy-Vehicle Test Methods-Part 4: Bulk Current Injection (BCI)*, std. ISO 11451-4: 1995(E).
[3] G. Cerri, R. De Leo, V. M. Primiani, S. Pennesi, and P. Russo, "Wide-Band characterization of current probes," *IEEE Trans. Electromagn. Compat.*, vol. 45, no. 4, pp. 616–625, Nov. 2003.
[4] N. Karrer and P. Hofer-Noser, "PCB Rogowski coils for high di/dt current measurements," in *Proc. Power Electronics Specialists Conf.*, vol. 3, 2000, pp. 1296–1301.
[5] C. E. Baum, "Some considerations for inductive current sensors: Note 59," in *Sensor and Simulation Notes (EMP 1) 1-422*, C. E. Baum, Ed.   Kirtland, NM: Air Force Research Labs., Directed Energy Directorate, 1999.
[6] F. Costa, E. Laboure, F. Forest, and C. Gautier, "Wide bandwidth, large AC current probe for power electronics and EMI measurements," *IEEE Trans. Ind. Electron.*, vol. 44, no. 4, pp. 502–511, Aug. 1997.
[7] A. Van den Bossche and J. Ghijselen, "EMC combined di/dt current probe," in *Proc. IEEE Int. Symp. Electromagnetic Compatibility*, vol. 2, Washington, DC, 2000, pp. 569–573.
[8] "Specifications for radio disturbance and immunity measuring apparatus and methods—Part 1: Radio disturbance and immunity measuring apparatus—measuring apparatus," CISPR 16-1, IEC:1999 + Admendment 1, 2002.
[9] A. R Ruddle, S. C. Pomeroy, and D. D. Ward, "Calibration of current transducers at high frequencies," *IEEE Trans. Electromagn. Compat.*, vol. 43, no. 1, pp. 100–104, Feb. 2001.
[10] J. Sroka, "Contribution of the target in the measurement uncertainty by calibration of the ESD generator," in *Proc. 14th Int. Zurich Symp. Electromagnetic Compatibility*, Feb. 2001, pp. 189–192.
[11] ——, "Measurement uncertainty of the target scattering parameters built in the uncertainty estimation of ESD simulator Sroka, J.," in *Proc. IEEE Int. Symp. Electromagnetic Compatibility*, vol. 2, Aug. 19–23, 2002, pp. 895–900.
[12] M. Beyer, W. Boeck, K. Moller, and W. Zaengl, *Hochspannungstechnik Theoretische und Praktische Grundlagen fur die Anwendug*.   New York: Springer-Verlag, 1986, pp. 319–319.
[13] R. A. Witte, *Electronic Test Instruments: Theory and Application*.   Englewood Cliffs, NJ: Prentice-Hall, 1993, ch. 1.14.

David Pommerenke (M'98–SM'04) was born on April 11, 1962, in Ann Arbor, MI. He received the Diploma in electrical engineering and the Ph.D. degree in transient fields of electrostatic discharge (ESD) from the Technical University of Berlin, Germany, in 1989 and 1995, respectively.

In 1989, he was a Research and Teaching Assistant at the Technical University of Berlin. He was with Hewlett Packard (HP) in 1996 and in 2001, he became associate a Professor in the Electromagnetic Compatibility Group, University of Missouri-Rolla. His areas of interest are EMC, ESD, numerical methods and calculation, high-voltage partial discharge detection systems, electronics and design of test and measurement equipment. He teaches classes in electronics, instrumentation, signal integrity and electromagnetics. Five of his patents have been issued.
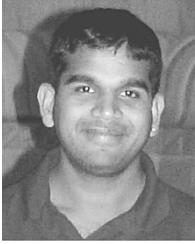
Ramachandran Chundru (M'04) was born in India in 1977. He received the B.S.E.E. degree from the University of Madras, India, in 2000 and the M.S.Comp.E. and M.S.E.E. degrees from the University of Missouri-Rolla, in 2001 and 2004, respectively.

From 2001 to 2004, he was with the Electromagnetic Compatibility Laboratory, University of Missouri-Rolla (UMR EMC Lab). He is currently working as a System Level ESD Engineer at Texas Instruments Incorporated, Dallas, TX. His research interests include ESD, EMC, signal integrity, high-voltage systems, as well as advanced RF Measurements.

Mr. Chundru is a Member of the ESD Association, WG 14, the working group that is standardizing the Cable Discharge Event (CDE).

Sunitha Chandra (M'04) was born in India in 1978. She received the B.S.E.E degree form Sri Krishna Devaraya University, India, in 2000 and the M.S.Comp.E. and M.S.E.E. degrees from the University of Missouri-Rolla, in 2002 and 2004, respectively.

From 2002 to 2004, she was with the Electromagnetic Compatibility Laboratory, University of Missouri-Rolla (UMR EMC Lab). She is currently working as a Signal Integrity Engineer with Nvidia Corporation, Santa Clara, CA. Her current research interests include signal integrity, EMC, and RF measurements.